

Tangential Flow Analysis of Giesekus Model in Concentric Annulus with Both Cylinders Rotation

M. Jouyandeh, M. Moayed Mohseni[†] and F. Rashidi

Department of Chemical Engineering, Amirkabir University of Technology, P.O. Box: 15875-4413, No. 472, Hafez Ave., Tehran, Iran

[†]Corresponding Author Email: m.moayed@aut.ac.ir

(Received August 10, 2016; accepted May 22, 2017)

ABSTRACT

Giesekus viscoelastic fluid is solved analytically for purely tangential flow in a concentric annulus at laminar and steady state conditions. Flow is created by a relative rotational motion between the cylinders. The analytical expressions for yield dimensionless velocity profile, pressure distribution, $f Re$ (f and Re are Fanning friction factor and Reynolds number) and material functions (viscosity, first and second normal stress difference coefficients) are obtained in cylindrical coordinates. Results show that difference between the values of lower as well as upper critical limits of the velocity ratio (where the minimum velocity happens) with their corresponding Newtonian values increase when mobility factor (α) and Deborah number (De) increase. The results also show that viscometric functions decrease by increasing elasticity because the viscoelastic fluid shows the shear thinning behavior which is strengthened by increasing elasticity. It is found that, for all De values, $f Re/f Re_N$ profiles are symmetrical around $\beta = 1/k$ (β and k are velocity ratio and radius ratio) because no relative motion exists.

Keywords: Giesekus model; Deborah number; Elasticity; Velocity ratio; Material functions.

1. INTRODUCTION

Flow induced in a concentric annulus by a relative rotational motion between the cylinders is used in many industries and engineering equipment; such as swirl nozzles, rotating electrical machines, standard commercial viscometers, rotating disks, journal bearings and other mechanical, biomechanical and chemical mixing equipment (Maron and Cohen, 1991). Giesekus (1982) is a three-parameters and nonlinear viscoelastic model which has been developed by using molecular ideas. The advantages of this model induce description of power-law regions for normal-stress coefficients and viscosity; reasonable complex and elongational viscosity. This model also incorporates non-exponential stress relaxation; shear-thinning shear viscosity; start-up curves and finite asymptotic value for extensional viscosity. An extensive literature review on the non-Newtonian fluids flow by inner cylinder rotating through concentric and eccentric annuli is given by Escudier *et al.* (2002). Velocity profiles of Newtonian fluid between two rotating cylinders for

different velocity ratios were investigated by Mahmud and Fraser (2003). Casson fluid flow was investigated between rotating cylinders by Batra and Eissa (1992). Rao (1999) studied Johnson-Segalman fluid flow between rotating cylinders. Beris *et al.* (1983) analyzed the tangential flow of CEF, Maxwell and White-Metzner fluids in concentric and eccentric annulus. Analytical solution for helical flow of SPTT fluids is derived in very thin annuli with inner cylinder rotating by Cruz and Pinho. (2004). Also, various hydrodynamic investigations were performed for tangential flow of viscoelastic fluids in eccentric annuli using numerical methods (Germann *et al.*, 2011; Beris *et al.*, 1987; Huang *et al.*, 1996). The investigation on the annular tangential flow of PTT viscoelastic fluid was presented by Mirzazadeh *et al.* (2005). Takht Ravanchi *et al.* (2007) obtained solution for flow by rotating inner cylinders in concentric annulus using the Giesekus model. It was expected to reproduce the results of Takht Ravanchi *et al.* (2007) by assuming the outer cylinder to be stationary, but by reconstruction of the aforementioned study the revealed error is

observed in the evaluation of $\tau_{\theta\theta}^*$ and $f Re$. In this study an analytical solution has been presented for purely tangential flow of Giesekus viscoelastic fluid in a concentric annulus when both cylinders are rotated with different angular velocities. This problem has not yet been addressed in literature. Also, the effect of velocity ratio on velocity profile, frictional factor, and pressure distribution has been reported.

2. GOVERNING EQUATIONS

The consideration of problem is steady state, laminar, and purely tangential flow. The no-slip condition is assumed. R_o and R_i are outer and inner cylinder radiuses with $R_i\Omega_i$ and $R_o\Omega_o$ as boundary conditions respectively. Also, the annular gap is defined as $\delta = R_o - R_i$.

By applying the assumptions, tangential and radial momentum equations are given as follows:

$$-\rho \frac{V_{\theta}^2}{r} = \frac{1}{r} \frac{\partial}{\partial r} (r\tau_{rr}) - \frac{\tau_{\theta\theta}}{r} - \frac{\partial p}{\partial r} \quad (1)$$

$$\frac{1}{r^2} \frac{\partial}{\partial r} (r^2 \tau_{r\theta}) = 0 \quad (2)$$

The Giesekus constitutive equation is as follows:

$$\tau + \frac{\alpha\lambda}{\eta} (\tau \cdot \tau) + \lambda \tau_{(1)} = \eta \dot{\gamma} \quad (3)$$

Where

$$\dot{\gamma} = [\nabla v + (\nabla v)^T] \quad (4)$$

$$\tau_{(1)} = \frac{\partial \tau}{\partial t} - \frac{D\tau}{Dt} - \{\tau \cdot \nabla v + (\nabla v)^T \cdot \tau\} \quad (5)$$

$$\frac{D\tau}{Dt} = \frac{\partial \tau}{\partial t} + (v \cdot \nabla) \tau \quad (6)$$

λ and η are model parameters representing zero-shear relaxation time and zero-shear viscosity, respectively (Giesekus, 1983). Also Eq.(3) defines the alpha parameter (α) which represents anisotropic hydrodynamic drag on the constituent polymer molecules and/or anisotropic Brownian motion (Bird *et al.*, 1987) and should be in the range of 0-1 ($0 \leq \alpha \leq 1$) as discussed by Giesekus (1982). By putting $\alpha = 0$ the model simplifies to the upper convected Maxwell. By introducing characteristic velocity ($V_c = R_i \Omega_i$), the Deborah number ($De = \lambda V_c / \delta$) which measures the fluid elasticity magnitude, characteristic shear stress ($\eta V_c / \delta$) and

$\dot{\gamma}^* = \frac{\dot{\gamma}}{V_c / \delta}$, the dimensionless form of constitutive equations will be as follows:

$$\tau_{rr}^* + \alpha De (\tau_{rr}^{*2} + \tau_{r\theta}^{*2}) = 0 \quad (7)$$

$$\tau_{r\theta}^* - De \dot{\gamma}^* \tau_{rr}^* + \alpha De \tau_{r\theta}^* (\tau_{rr}^* + \tau_{\theta\theta}^*) = \dot{\gamma}^* \quad (8)$$

$$\tau_{\theta\theta}^* - 2De \dot{\gamma}^* \tau_{r\theta}^* + \alpha De (\tau_{r\theta}^{*2} + \tau_{\theta\theta}^{*2}) = 0 \quad (9)$$

By integrating Eq.(2) dimensionless shear stress ($\tau_{r\theta}^*$) can be obtained as follows:

$$\tau_{r\theta}^* = \frac{k^2 \tau_{wi}^*}{r^{*2}} \quad (10)$$

Where τ_{wi}^* is dimensionless inner wall shear stress, r^* is r/R_o and k is the radius ratio (R_i/R_o).

By solving Eq.(7) in terms of τ_{rr}^* as follows:

$$\tau_{rr}^* = \frac{-1 \pm \sqrt{1 - 4\alpha^2 De^2 \tau_{r\theta}^{*2}}}{2\alpha De} \quad (11)$$

By solving Eq.(7) the positive and negative solution obtain which is obvious in Eq.(11). Schleiniger and Weinacht (1991) by using linear stability analysis represent the following restrictions when Giesekus fluid is considered without solvent.

For positive solution:

$$|\tau_{r\theta}^*| < \frac{1}{De} \sqrt{\frac{1}{\alpha} - 1} \quad 0 < \alpha \leq \frac{1}{2} \quad (12-a)$$

$$|\tau_{r\theta}^*| \leq \frac{1}{2\alpha De} \quad \frac{1}{2} < \alpha \leq 1 \quad (12-b)$$

For negative solution:

$$\frac{1}{De} \sqrt{\frac{1}{\alpha} - 1} < |\tau_{r\theta}^*| \leq \frac{1}{2\alpha De} \quad \frac{1}{2} < \alpha \leq 1 \quad (13)$$

As a result of restrictions the positive solution was concluded for solving process.

From Eq.(8), the following expression can be obtained:

$$\tau_{\theta\theta}^* = \frac{1 + De \tau_{rr}^*}{\alpha De \tau_{r\theta}^*} \dot{\gamma}^* - \frac{1 + \alpha De \tau_{rr}^*}{\alpha De} \quad (14)$$

Combining Eqs.(7), (9) and (14) leads to:

$$\dot{\gamma}^* = (1-k)r^* \frac{\partial}{\partial r^*} \left(\frac{V_{\theta}^*}{r^*} \right) = \frac{1 + (2\alpha - 1)De \tau_{rr}^*}{(1 + De \tau_{rr}^*)^2} \tau_{r\theta}^* \quad (15)$$

By substituting Eq.(11) and Eq.(15) into Eq.(14), the simplified tangent normal stress can be obtained:

$$\tau_{\theta\theta}^* = \frac{(\alpha - 1)(-1 \pm \sqrt{1 - 4\alpha^2 De^2 \tau_{r\theta}^{*2}}) + 2\alpha^2 De^2 \tau_{r\theta}^{*2}}{\alpha De (2\alpha - 1 \pm \sqrt{1 - 4\alpha^2 De^2 \tau_{r\theta}^{*2}})} \quad (16)$$

By consideration an approximate solution

approaches, the term $\sqrt{1-4\alpha^2 De^2 \tau_{r\theta}^{*2}}$ in Eqs.(11) and (16) can be expressed by a power series. For the small amounts of $4\alpha^2 De^2 \tau_{r\theta}^{*2}$, the first two terms of series are presented and higher order terms can be cut off (Moayed Mohseni and Rashidi (2015), Takht Ravanchi *et al.* (2007) and Mirzazadeh *et al.* (2005)):

$$\sqrt{1-4\alpha^2 De^2 \tau_{r\theta}^{*2}} \cong 1-2\alpha^2 De^2 \tau_{r\theta}^{*2} \quad (17)$$

The resulting error of this approximate for $4\alpha^2 De^2 \tau_{r\theta}^{*2} < 1/2$ (or $|\tau_{wi}^*| < \frac{1}{2\sqrt{2}\alpha De}$) is less than 6%. It should be noted that besides satisfaction of validity condition of the approximate, the stability condition (Eq. (12) or (13)) should also be established.

Substituting Eq.(17) in Eq.(16) gives:

$$\tau_{\theta\theta}^* = \frac{-\alpha De \tau_{r\theta}^{*2} + 2De \tau_{r\theta}^{*2}}{1-\alpha De^2 \tau_{r\theta}^{*2}} \quad (18)$$

Using a similar approximation, the equation for τ_{rr}^* becomes:

$$\tau_{rr}^* = -\alpha De \tau_{r\theta}^{*2} \quad (19)$$

Substituting $\tau_{r\theta}^*$ and τ_{rr}^* from Eqs.(10) and (19) in to Eq. (15) and integration, the dimensionless velocity profile

is derived as follows:

$$\frac{V_\theta^*}{r^*} = \frac{1}{4} \left(\frac{A}{B} - 1 \right) \frac{k^2 \tau_{wi}^*}{1-k} \frac{r^{*2}}{r^{*4} - B \tau_{wi}^{*2}} - \frac{1}{4} \frac{k^2}{\sqrt{B}(1-k)} \left(1 + \frac{A}{B} \right) \arctan h \left(\frac{r^{*2}}{\tau_{wi}^* \sqrt{B}} \right) + C \quad (20)$$

Where

$$A = \alpha(2\alpha-1)De^2 k^4 \quad (21)$$

$$B = \alpha De^2 k^4 \quad (22)$$

By imposing the following dimensionless boundary conditions, the constant (C) of Eq.(20) can be obtained.

$$V_\theta^* = 1 \quad r^* = k \quad (23)$$

$$V_\theta^* = \beta \quad r^* = 1 \quad (24)$$

The velocity ratio (β) is defined as $R_o \Omega_o / R_i \Omega_i$.

Also by introducing the boundary conditions into Eq.(20) the following relation is obtained.

$$\frac{1}{k} - \beta = \frac{k^2 \tau_{wi}^*}{4(1-k)} \left(\frac{A}{B} - 1 \right) \left[\frac{k^2}{k^4 - B \tau_{wi}^{*2}} \right] - \frac{k^2}{4\sqrt{B}(1-k)} \left(\frac{A}{B} + 1 \right) \left[\arctan h \left(\frac{k^2}{\tau_{wi}^* \sqrt{B}} \right) - \arctan h \left(\frac{1}{\tau_{wi}^* \sqrt{B}} \right) \right] \quad (25)$$

Now, τ_{wi}^* can be obtained from the strongly nonlinear Eq. (25). Newton-Raphson method was used to solve of this equation.

Torque friction factor is defined below:

$$f = \frac{\tau_w}{\rho V_c / 2} \quad (26)$$

when torque friction factor is combined with rotational Reynolds number ($Re = \rho V_c \delta / \eta$), a recent group is created as follows:

$$f Re = 2\tau_{wi}^* \quad (27)$$

The pressure variation through the annulus gap is evaluated. The dimensionless form of Eq.(1) is as follows:

$$\frac{\partial p^*}{\partial r^*} = Re \frac{V_\theta^{*2}}{r^*} + \frac{1}{r^*} \frac{\partial}{\partial r^*} (r^* \tau_{rr}^*) - \frac{\tau_{\theta\theta}^*}{r^*} \quad (28)$$

The dimensionless pressure is defined as $(p/(\eta V_c / \delta))$. The pressure variation across the annulus slot can be obtained by integration of this equation. By introducing $\tau_{\theta\theta}^*$ from Eq. (18), τ_{rr}^* from (19), $\tau_{r\theta}^*$ from Eq.(10), and V_θ^* from Eq.(20) into Eq.(28) and then integrating the analytical expression for the radial pressure distribution is derived as follows:

$$p^* - p_i^* = \phi(r^*) - \phi(k) \quad (29)$$

Where $\phi(r^*)$ is:

Where $h = \text{Arc tanh} \left(\frac{r^{*2}}{\tau_{wi}^* \sqrt{B}} \right)$ and (C) is the constant of integration in velocity profile.

3. MATERIAL FUNCTIONS

The apparent viscosity for non-Newtonian fluids which is depended on the shear rate is defined as follows (Bird *et al.*, 1987):

$$\mu(\dot{\gamma}^*) = \frac{\tau_{r\theta}^*}{\dot{\gamma}^*} \quad (31)$$

By putting Eq. (19) in Eq.(15) a nonlinear equation for $\tau_{r\theta}^*$ is obtained. By solving it and then some mathematical simplification, $\tau_{r\theta}^*$ is obtained as a function of $\dot{\gamma}^*$ (Eq. (32)).

$$\phi(r^*) = \frac{1}{128} \left(\begin{aligned} & 64C^2 r^{*2} \operatorname{Re} \left[\frac{16(A+B)Ch^2 k^2 \operatorname{Re} \tau_{wi}^*}{B(k-1)} - \frac{96Dk^4 \alpha \tau_{wi}^{*2}}{r^{*4}} + \frac{2(A-B)^2 k^4 \operatorname{Re} \tau_{wi}^{*2}}{B^2 (k-1)^2 (-r^{*4} + B\tau_{wi}^2)} \right] \\ & + \frac{16(A+B)Ck^2 \operatorname{Re} \left(-2hr^{*2} + \sqrt{B}h^2 \tau_{wi} - \sqrt{B} \tau_{wi} \operatorname{Log} \left[1 - r^{*4} / B\tau_{wi}^2 \right] \right)}{B^{3/2} (k-1)} - \frac{32(-2+\alpha) \operatorname{Log} \left[r^{*4} / (r^{*4} - B\tau_{wi}^2) \right]}{\alpha De} \\ & + \frac{(A-B)k^2 \operatorname{Re} \tau_{wi} \left((A-B)k^2 \operatorname{Log} \left[(r^2 - \sqrt{B} \tau_{wi}) / (r^2 + \sqrt{B} \tau_{wi}) \right] - 16B^{3/2} C(k-1) \operatorname{Log} \left[r^4 - B\tau_{wi}^2 \right] \right)}{B^{3/2} (k-1)^2} \\ & + \frac{4(A+B)k^4 \operatorname{Re} \left(h(Ar^2 + Br^2 - 2B^{3/2} \tau_{wi}) - 4B^{3/2} \tau_{wi} \operatorname{Log} [1 + e^{-2h}] \right) + 2B^{3/2} \tau_{wi} \operatorname{PolyLog} \left[\frac{2}{3}, -e^{-2h} \right]}{B^3 (k-1)^2} \end{aligned} \right) \quad (30)$$

$$\tau_{r\theta}^* = \frac{\dot{\gamma}^* (1 + 2III + \sqrt{II})}{4 \times I} - \frac{(1 - 2\alpha) \sqrt{III + De^2 (1 + 4III) \dot{\gamma}^{*2} + (De^2 \dot{\gamma}^{*2} - III) \sqrt{II}}}{2\sqrt{2} De \times I} \quad (32)$$

$$I = \alpha \left((1 - 2\alpha)^2 + \dot{\gamma}^{*2} De^2 \right)$$

$$II = 1 - 16De^2 (\alpha - 1) \alpha \dot{\gamma}^{*2} \quad III = 4\alpha (\alpha - 1)$$

Substituting Eq.(32) into Eq.(31) results in the non-Newtonian viscosity of Giesekus model. Likewise we can define first and second normal stress difference coefficients ψ_1 and ψ_2 for tangential flow as follows:

$$\psi_1(\dot{\gamma}^*) = \frac{\tau_{\theta\theta}^* - \tau_{rr}^*}{\dot{\gamma}^{*2}} = \frac{\alpha De \tau_{r\theta}^{*2} + \frac{De(\alpha - 2) \tau_{r\theta}^{*2}}{\alpha De^2 \tau_{r\theta}^{*2} - 1}}{\dot{\gamma}^{*2}} \quad (33)$$

$$\psi_2(\dot{\gamma}^*) = \frac{\tau_{rr}^* - \tau_{zz}^*}{\dot{\gamma}^{*2}} = -\frac{\alpha De \tau_{r\theta}^{*2}}{\dot{\gamma}^{*2}} \quad (34)$$

ψ_1 and ψ_2 are determined by putting $\tau_{r\theta}^*$ in Eqs.(33) and (34). The parameters μ , ψ_1 and ψ_2 are collectively referred to as the viscometric functions.

At low shear rates, viscometric functions approach the limiting values of μ , ψ_1 and ψ_2 which are referred to as the zero shear rate viscosity (η), the zero shear rate first normal stress coefficient ($\psi_{1,0}$), and the zero shear rate second normal stress coefficient ($\psi_{2,0}$) respectively (Bird *et al.*, 1987).

$$\lim_{\dot{\gamma} \rightarrow 0} \mu = \eta \quad \lim_{\dot{\gamma} \rightarrow 0} \psi_1 = \psi_{1,0} \quad \lim_{\dot{\gamma} \rightarrow 0} \psi_2 = \psi_{2,0} \quad (35)$$

Figure 1 shows the verification of the results obtained from Eqs.(32-34) with the normalized experimental data.

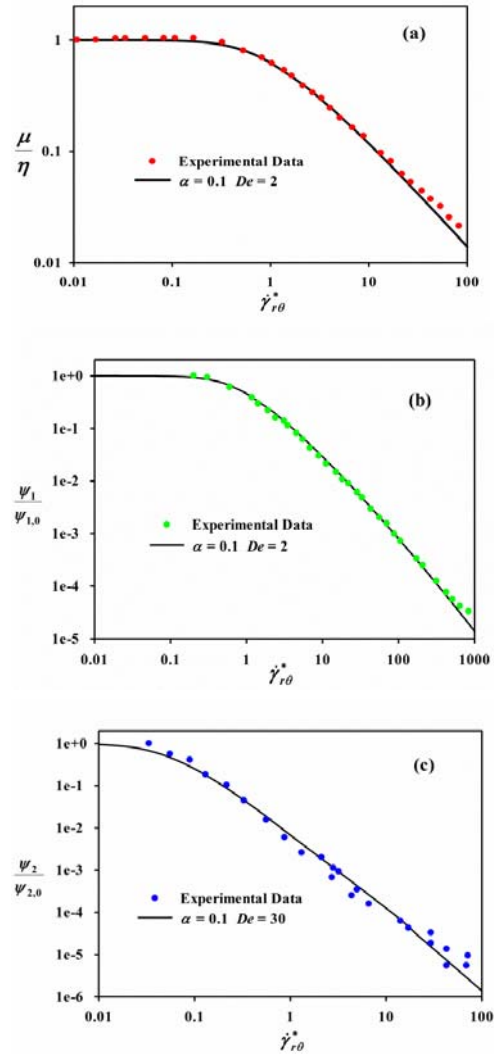


Fig. 1. comparison of (a) normalized viscosity of model with 7% solution of aluminum laurate in a mixture of decalin and m-cresol (Bird *et al.*, 1987, p. 106) (b) normalized first normal stress difference coefficient of model with 1.5% solution of polyacrylamide (Separan AP30) in a water glycerin mixture (Bird *et al.*, 1987, p.108) (c) normalized second normal stress difference coefficient of model with 2.5% solution of polyacrylamide in a 50/50 mixture of water and glycerin (Bird *et al.*, 1987, p. 110).

4. RESULTS AND DISCUSSION

Figures 2a-c show the effects of shear rate and elasticity on the viscometric functions (μ , ψ_1 and ψ_2) which are normalized with the limiting values. It is seen at low shear rates the normalized viscometric functions approach unity. Also, viscometric functions decrease with increasing shear rate and elasticity because the viscoelastic fluid shows the shear thinning behavior which is strengthened by increasing elasticity. Fig. 3 shows the velocity ratio (β) effect on velocity profile. The shape of velocity profile depends on β value. β will be positive for the same direction rotation of both cylinders and negative for opposite direction rotation of them. $\beta = 0$ means that outer wall is at rest. As can be seen from this figure, a minimum point is shown on the velocity distribution for a range of critical velocity ratio (β_c) i.e. $\beta_{c,lower} \leq \beta \leq \beta_{c,upper}$. The lower and upper values of β_c can be determined by Letting $r_{min}^* = 1$ and $r_{min}^* = k$ in Eq.(36), (in this figure for $r_{min}^* = 0.5$ and $r_{min}^* = 1$ the lower and upper critical β have been obtained respectively as: $\beta_{c,lower} = 0.641732$ and $\beta_{c,upper} = 1.36477$. Velocity increases along the radial direction for $\beta > \beta_{c,upper}$. Velocity decreases for $0 \leq \beta < \beta_{c,lower}$, and its value becomes β at the outer wall. For $\beta < 0$, where cylinders are in counter-rotating motion, velocity becomes zero somewhere in the radial position.

The minimum velocity location has obvious importance in the second law of thermodynamics analysis because at this point the entropy generation disappears due to fluid friction. (Mahmud and Fraser, 1987).

$$\frac{\partial V_{\theta}^*}{\partial r^*} = \frac{(\frac{A}{B}-1)k^2 r^{*2} \tau_{wi}^*}{4(k-1)(r^{*4} - B\tau_{wi}^{*2})} + r^* \frac{(k^2 \tau_{wi}^* (A\tau_{wi}^{*2} r^* - r^{*5}))}{(k-1)(r^{*4} - B\tau_{wi}^{*2})^2} - \frac{(\frac{A}{B}+1)k^2 \text{Arctanh}(\frac{r^{*2}}{\tau_{wi}^* \sqrt{B}})}{4\sqrt{B}(1-k)} + c = 0 \quad (36)$$

the minimum velocity location is obtained by solving Eq. (36). Since this equation is highly nonlinear, inevitably, the Newton-Raphson method is employed. The location of minimum velocity i.e. (r_{min}^*), which is normalized with the corresponding Newtonian value ($r_{min,N}^* = \sqrt{k(k\beta - 1)/(k - \beta)}$), as a function of De number is shown in Fig. 4. As can be seen, $r_{min}^*/r_{min,N}^*$ departs further from Newtonian fluid by increasing fluid elasticity. The effect of Deborah number and radius ratio k on $\beta_{c,lower}/\beta_{c,N}$ is shown in Fig. 5 where $\beta_{c,N}$ is Newtonian velocity ratio

which defined as $\beta_{c,lower,N} = 2k/(1+k^2)$. For thin annulus ($k=0.9$), there is only a slight difference between β_c and the corresponding Newtonian value and therefore it is not affected by elasticity. But for small radius ratios for example $k = 0.1$, this difference is significant. Fig. 6 shows the effect of mobility factor (α) on $\beta_{c,upper}$ which is normalized with the corresponding Newtonian value ($\beta_{c,upper,N} = (1+k^2)/2k$). As can be seen, this value increases by increasing α and De . Fig. 7 shows the effect of fluid elasticity on normal-stress, which is normalized with inner wall shear stress. The existence of normal stresses in polymeric systems is due to the anisotropy induced in the microstructure because of flow. Since the anisotropy of polymer solution increases by increasing elasticity therefore, it causes high normal stresses, which is clearly seen in Fig. 7.

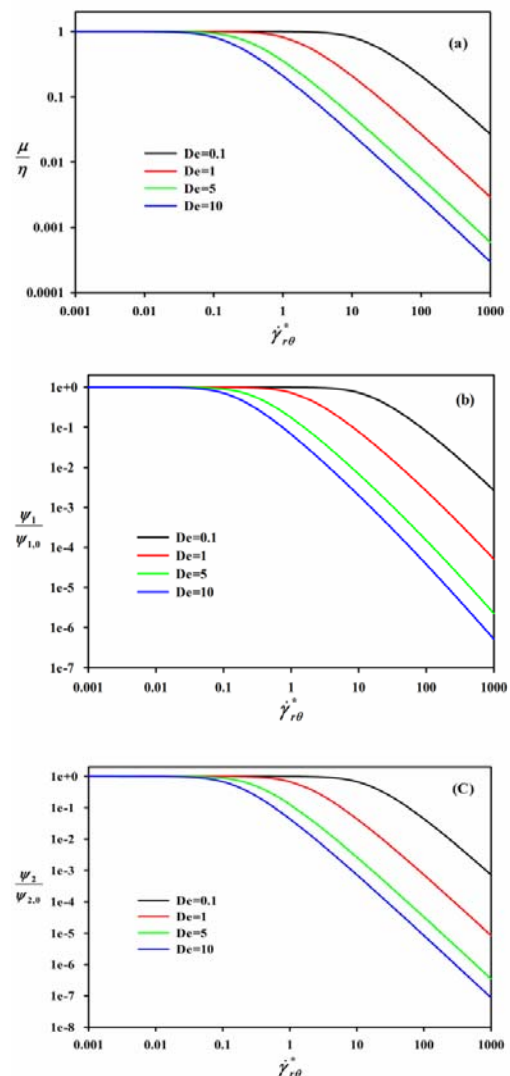


Fig. 2. Effect of elasticity on the normalized (a) non-Newtonian viscosity, (b) first normal stress difference coefficient, (c) second normal stress difference coefficient with dimensionless shear rate for a Giesekus fluid for $\alpha = 0.1$.

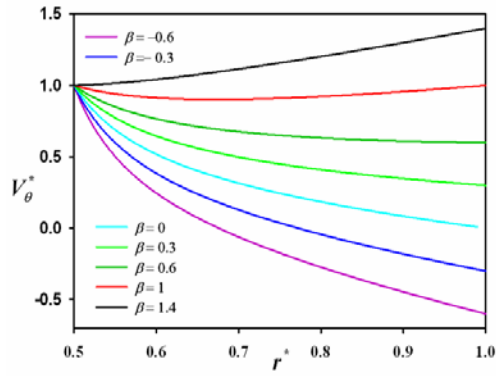


Fig. 3. Dimensionless velocity profiles with varying velocity ratio (β) for $\alpha = 0.2$, $k = 0.5$, $De = 0.5$.

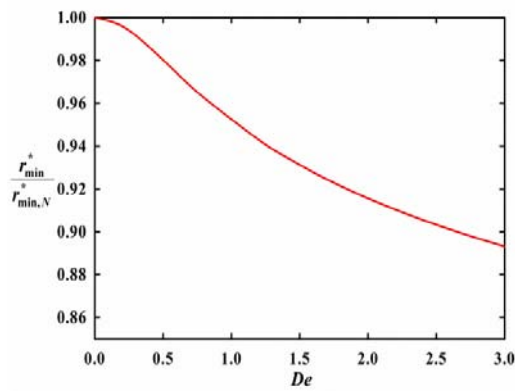


Fig. 4. $r_{min}^*/r_{min,N}^*$ versus Deborah number (De) for $\alpha = 0.2$, $k = 0.5$ and $\beta = 1$.

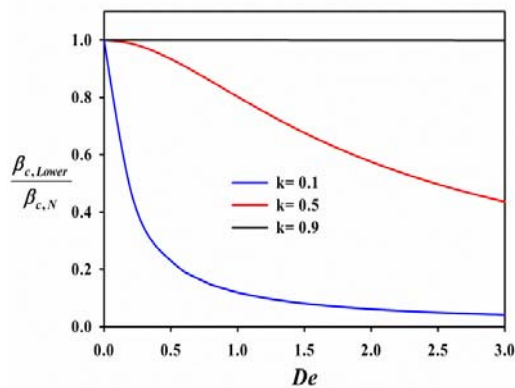


Fig. 5. $\beta_{c,lower}/\beta_{c,N}$ versus Deborah number (De) and radius ratio (k) for $\alpha = 0.2$.

A similar convex pattern is observed in Fig. 8. For each k value, profile is again symmetrical around $\beta = 1/k$, when the cylinders are stationary relative to each other, i.e. $\Omega_o = \Omega_i$. Figs. 9a-c shows pressure variations with elasticity and centrifugal force. For low values of Re (e.g. $Re=1$) the centrifugal force is negligible. Therefore, in Fig. 9a

only the effect of elasticity becomes important. By rewriting Eq.(1) can be derive Eq.(37) as follows (Mirzazadeh *et al.*,2007):

$$\frac{\partial p}{\partial \ln r} = \rho V_{\theta}^2 - (\tau_{\theta\theta} - \tau_{rr}) - 2\tau_{r\theta} \frac{\partial \tau_{rr}}{\partial \tau_{r\theta}} \quad (37)$$

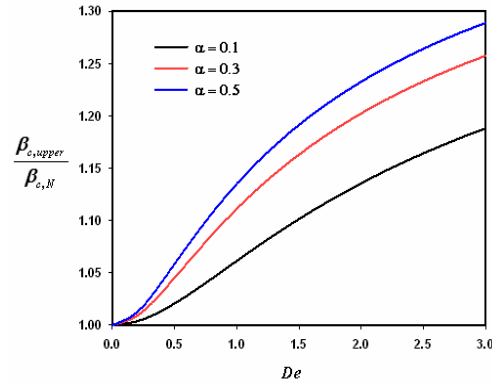


Fig. 6. $\beta_{c,upper}/\beta_{c,N}$ versus Deborah number (De) and mobility factor (α) for $k = 0.5$.

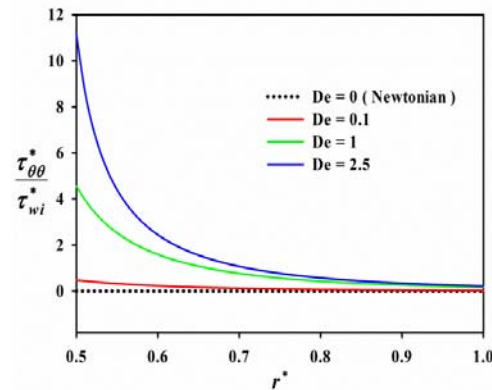


Fig. 7. Normalized dimensionless normal stress profile with varying De for $\alpha = 0.2$, $k = 0.5$ and $\beta = 0$.

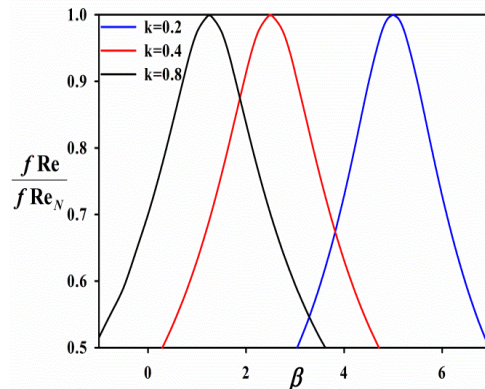


Fig. 8. $f Re/f Re_N$ versus velocity ratio (β) for $\alpha = 0.2$, $De = 1$ and different values of k .

For Newtonian fluids the first and second normal

stress differences are both zero in shear flow and therefore, pressure increases with the increase of radius as can be seen in Fig.9a.

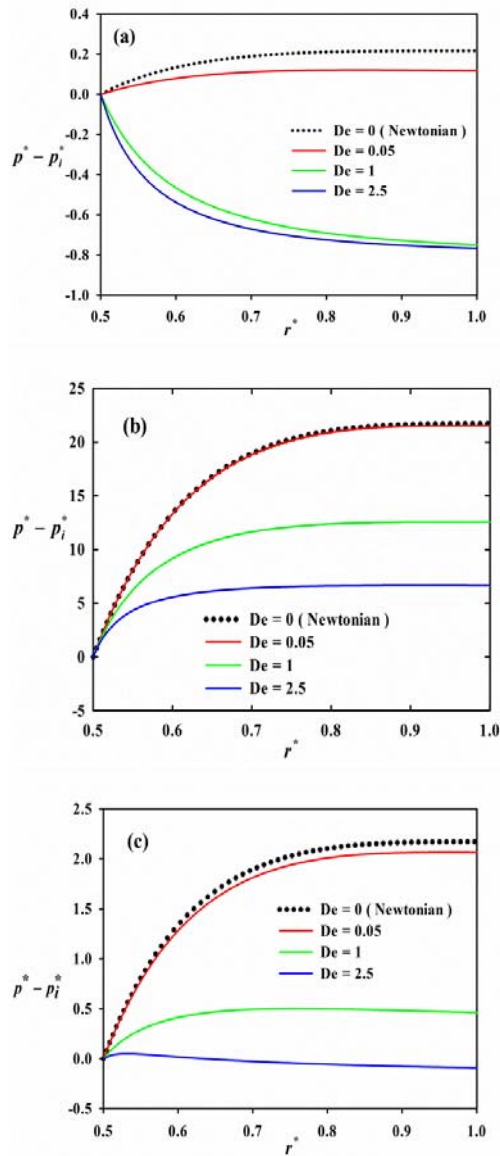


Fig. 9. Pressure variations versus Deborah number (De) with $k = 0.5$, $\alpha = 0.2$ and $\beta = 0$: (a) $Re = 1$ (b) $Re = 100$ (c) $Re = 10$.

For viscoelastic fluids first normal stress differences is practically always negative with an absolute value much larger than second normal stress differences. For this case pressure decreases in the radial direction as shown in Fig. 9a. Also, as can be seen in Fig. 7 by increasing the fluid elasticity the normal stresses increase. Hence, increasing fluid elasticity increases pressure variation across the annulus slot.

Figure 9b shows the effect of centrifugal force on pressure profile for high range of Re number (e.g. $Re = 100$). In this case centrifugal force dominates therefore first and second normal stress differences will be negligible, similar to Newtonian fluid and only the

first term of Eq.(37) remains. It is seen that increasing the elasticity reduces the pressure variation across the annulus slot because increasing elasticity decreases velocity in each location of annular space.

In Fig. 9c ($Re = 10$) centrifugal force and normal stress are both important. The results of Fig. 9c for low and high fluid elasticity are similar to Fig. 9b and Fig. 9a, respectively. For intermediate Deborah number (e.g. $De = 2.5$), the combination of normal stress difference and centrifugal force causes a maximum.

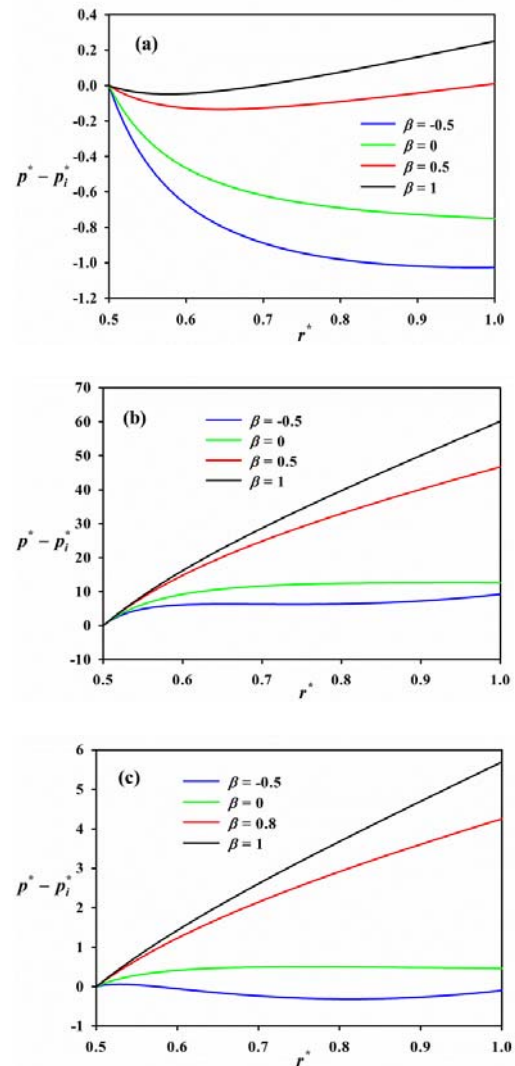


Fig. 10. Pressure variations versus velocity ratio (β) with $\alpha = 0.2$, $De = 1$ and $k = 0.5$ (a) $Re = 1$ (b) $Re = 100$ (c) $Re = 10$.

Figures 10a-c presents the effect of velocity ratio (β) on the pressure variations within the annulus slot. Fig. 10a shows that for $Re = 1$ the pressure distribution has a minimum for $\beta_{c,lower} \leq \beta \leq \beta_{c,upper}$. Also, for $\beta < \beta_{c,lower}$ pressure variation across the annulus slot is decreased but this trend is reversed

for $\beta > \beta_{c,upper}$. The Figs. 10-a and 10-b show that increasing radial pressure difference is always occurred expected for $\beta < 0$ and $Re = 10$.

5. CONCLUSIONS

The flow of Giesekus viscoelastic fluid model inside a laminar, steady state and tangential flow through an annulus by a relative rotational motion between the cylinders has been studied analytically. Results show that:

- Increasing shear rate and elasticity cause decreasing viscometric functions which indicates the shear thinning behavior of the viscoelastic fluid.
- Velocity profiles for $\beta > \beta_{c,upper}$ have positive slope, while they have negative slope for $\beta < \beta_{c,lower}$.
- For $\beta_{c,lower} \leq \beta \leq \beta_{c,upper}$ the velocity profile has a minimum, along the radius.
- The value of critical velocity ratio compared to their Newtonian counterparts increases by increasing fluid elasticity.
- Normal stress increases by increasing fluid elasticity due to the anisotropic microstructure.
- For $\beta = 1/k$, no relative angular motion exist. As a result, $f Re/f Re_N$ shows a symmetrical shape.
- By increasing fluid elasticity, $f Re/f Re_N$ decreases for different values of β .

REFERENCES

Batra, R. L. and B. Das (1992). Flow of Casson fluid between two rotating cylinder. *Fluid Dynamics Research* 7(1-3), 133–141.

Beris, A. N., R. C. Armstrong and R. A. Brown (1983). Perturbation theory for viscoelastic fluids between eccentric rotating cylinders. *Journal of Non-Newtonian Fluid Mechanics* 13(2), 109–143.

Beris, A. N., R. C. Armstrong and R. A. Brown (1987). Spectral/finite-element calculations of the flow of a Maxwell fluid between eccentric rotating cylinders. *Journal of Non-Newtonian Fluid Mechanics* 22(2), 129-167.

Bird, R. B., R. C. Armstrong, O. Hassager (1987). *Dynamics of polymeric liquids, second ed. Fluid Dynamics*, vol. 1, John Wiley, New York, USA.

Cruz, D. O. A. and F. T. Pinho (2004). Skewed Poiseuille–Couette low of SPTT fluids in concentric annuli and channels. *Journal of Non-Newtonian Fluid Mechanics* 121(1), 1–14.

Escudier, M. P., P. J. Oliveira and F. T. Pinho (2002). Fully developed laminar flow of purely viscous non-Newtonian liquids through annuli

including the effects of eccentricity and inner cylinder rotation. *International Journal of Heat and Fluid Flow* 23(1), 52–73.

Germann, N., M. Dressler and E. J. Windhab (2011). Numerical solution of an extended White–Metzner model for eccentric Taylor–Couette flow. *Journal of Computational Physics* 230(21), 7853–7866.

Giesekus, H. (1982). A simple constitutive equation for polymer fluids based on the concept of deformation-dependent tensorial mobility. *Journal of Non-Newtonian Fluid Mechanics* 11, 69–109.

Giesekus, H. (1983). Stressing behavior in simple shear flow as predicted by a new consecutive model for polymer fluids. *Journal of Non-Newtonian Fluid Mechanics* 12, 367–374.

Huang, X. and N. Phan-Thien (1996). Viscoelastic flow between eccentric rotating cylinders: unstructured control volume method. *Journal of Non-Newtonian Fluid Mechanics* 64(1), 71-92.

Jouyandeh, M., M. Moayed Mohseni and F. Rashidi (2014). Forced Convection Heat Transfer of Giesekus Viscoelastic Fluid in Concentric Annulus with both Cylinders Rotation. *Journal of Petroleum Science and Technology* 4(2), 1–9.

Mahmud, S. and R. A. Fraser (2003). Analysis of entropy generation inside cylindrical annuli with relative rotation. *International Journal of Thermal Science* 42(5), 513–521.

Maron, D. M. and S. Cohen (1991). Hydrodynamics and heat/mass transfer near rotating surfaces. *Advances in Heat Transfer* 21, 141–183.

Mirzazadeh, M., F. Rashidi and S. H. Hashemabadi (2005). Purely tangential flow of a PTT-viscoelastic fluid within a concentric annulus. *Journal of Non-Newtonian Fluid Mechanics* 129(2), 88–97.

Moayed Mohseni, M. and F. Rashidi (2010). Viscoelastic fluid behavior in annulus using Giesekus model. *Journal of Non-Newtonian Fluid Mechanics* 165(21-22), 1550–1553.

Mohseni, M., Rashidi, F. (2015). Axial annular flow of a Giesekus fluid with wall slip above the critical shear stress. *Journal of Non-Newtonian Fluid Mechanics* 223, 20–27

Rao, I. J. (1999). Flow of a Johnson–Segalman fluid between rotating coaxial cylinders with and without suction. *International Journal of Non-Linear Mechanics* 34(1), 63–70.

Schleiniger, G. and R. Weinacht (1991). Steady Poiseuille flows for a Giesekus fluid. *Journal of Non-Newtonian Fluid Mechanics* 40(1), 79–102.

Takht Ravanchi, M., M. Mirzazadeh and F. Rashidi (2007). Flow of Giesekus viscoelastic fluid in a concentric annulus with inner cylinder rotation. *International Journal of Heat and Fluid Flow* 28(4), 838–845.

